On Shortening the Effective mmWave MIMO Channel Impulse Response

Nikola Vučić, Marcin Iwanow, Mario H. Castañeda Garcia, Jian Luo, and Wen Xu
Huawei Technologies Duesseldorf GmbH, German Research Center
Riesstr. 25C, 80992 Munich, Germany
Email: {nikola.vucic, iwanow.marcin, mario.castaneda, jianluo, wen.dr.xu}@huawei.com

***Abstract*—mmWave communication typically resorts to beamforming in order to overcome the unfavorable propagation conditions in the high frequency bands. The directional transmission established using beamforming is beneficial also in terms of reducing the effective channel impulse response (CIR) and, correspondingly, the required guard periods in a block transmission scheme. While this effect has been investigated in the literature for the single stream case, in this paper we analyse the shortening of the effective multiple-input, multiple-output (MIMO) channel impulse response in a mmWave multistream transmission. It is shown that even though the complete effective MIMO channel impulse response might be relatively long, smart time delaying of streams sent over different physical paths can exploit the sparsity of the mmWave channel in the temporal-angular domain, and result in significant CIR shortening. In this way, guard period reduction can be achieved, with the overhead approaching that of the single stream case.**

I. Introduction

Exploitation of mmWave frequencies is an attractive approach to satisfy the ever increasing data rate demands in wireless communications, as there are large portions of underutilized spectrum in these bands [1]. However, there exist several new aspects related to communication in the mmWave spectrum compared with conventional sub-6 GHz cellular systems. In order to combat the high path loss in mmWave channels, more directional transmission is utilized by applying beamforming (BF) with large antenna arrays. mmWave channels exhibit further specific features such as a certain degree of sparsity and a fast time-varying nature. In addition, the increased sampling frequency due to large utilized bandwidths impacts the transceiver (TRX) architecture design particularly in terms of reducing the power consumption.

The setup that we consider can be briefly described as follows. We work with an instance of a general two-stage multiple-input multiple-output (MIMO) architecture for a multistream mmWave transmitter (Tx) and receiver (Rx). In both Tx and Rx, one processing stage is performing frequency independent BF. The other stage at the Rx is adaptive to instantaneous channels and has a full digital signal processing capability, while Tx is simplified and works with partial channel state information (CSI). This setup is of high practical interest, as channel estimation in mmWave systems is an intricate problem due to the very large antenna arrays involved and the rapidly changing mmWave channels.

A. Main Contributions

Similarly to other commercially used wireless systems, we employ block based transmission, having redundant symbols which guarantee no interblock interference due to the multipath wireless channel. The amount of redundancy to be added corresponds to the effective mmWave channel delay spread, where the effective channel assumes the physical wireless channel transformed through Tx/Rx BF. In mmWave MIMO transmission, different data streams can travel over very different physical paths. Therefore, the resulting MIMO channel impulse response might still be quite long if standard beamforming techniques are applied. To deal with this, large guard periods (GPs) are usually needed. The main contributions of this paper are in resolving this problem and can be summarized as follows:

- We propose a semi-open loop transmission mode where the Tx has only spatial information about different dominant paths and the corresponding transmission delays.
- The Tx streams are sent using different beams corresponding to different spatial lobes.
- The streams are conveniently delayed at the Tx so that they arrive approximately simultaneously at the Rx.
- The Rx has spatial information about the dominant paths and aligns its beams accordingly. In addition, the Rx applies a MIMO equalization algorithm on the effective channel to mitigate the interstream interference.
- The performance is evaluated using a statistical multipath mmWave channel model.

By aligning the arrival times of different symbols at the Rx, the proposed scheme shortens the effective MIMO channel impulse response (CIR) and enables a significant reduction in the overhead for elimination of the interblock interference. For example, with the considered model and when orthogonal frequency division multiplexing (OFDM) is concerned, the cyclic prefix (CP) length can be reduced more than ten times for a very large range of signal-to-noise (SNR) ratios of operational interest in mmWave communications.

B. Related Works

The topic of frequency selective MIMO channel shortening has drawn considerable attention in the past, particularly in the context of assisting equalization and detection techniques at the Rx [2]–[5]. Differently from these works, our aim is

ISBN 978-3-8007-4394-0

to exploit some properties specific for the mmWave channel in order to design a very simple and robust channel shortening method at the Tx, rather then employing sophisticated equalizers for this purpose.

In the IEEE 802.11ad (license free, 60 GHz WiFi) standard, both single carrier (SC) and OFDM block transmission modes are supported [6]. Tx and Rx BF are included in the specification, as well. However, multistream MIMO communication is about to be treated only in the future version of this standard. It should be remarked that 3GPP intends to embrace communication in high frequency bands already in the first release of the future 5G cellular standard, though the details are yet to be specified [7].

In [8], MIMO OFDM transceiver design for mmWave communication is studied. However, different from the work at hand, no particular characteristics of the directional transmission required for mmWave links are exploited for reduction of the channel delay spread.

The work [9] proposes a delay compensation method at the transmitter for mmWave communication systems. However, only single stream transmission is supported by this scheme, and no direct extension for a multi-stream transceiver is obvious. Further, each channel cluster is assumed to be frequency flat, which might not always be the case in practice.

A system based on lens antenna arrays is utilized in [10], with path grouping and delaying with MIMO processing for spatially irresolvable groups. This solution requires a specific type of antenna array and it is not applicable in general to the hybrid beamforming or two stage approaches considered here.

Finally, time reversal methods assume matched pre-filtering at the Tx (cf., e.g., [11]), so delaying at the Tx is implicitly performed. The work [12] applies time reversal to mmWave communications. The main differences from the proposed solution are in the fact that complete channel information is needed at the Tx for the time reversal schemes. Further, spectrally efficient transmission in the sense of reducing the relevant CIR length is not elaborated in these reference works.

C. Notation

Matrices and vectors are denoted by large and small bold letters, respectively. $(\cdot)^{\mathrm{H}}$ and $\|(\cdot)\|$ denote the conjugate transpose and the Euclidean vector norm, respectively.

II. System Model and Problem Statement

Our main focus is on the point-to-point transmission, as illustrated in Fig. 1. The transmitter (Tx) is a base station (BS), while the receiver (Rx) is an end user device (in downlink transmission) or another BS (in a backhaul type of link). We assume that the Tx is equipped with a large antenna array of N_t antenna elements, which enables it to create sharp beams (gray shaded in Fig. 1), while the Rx has N_r antenna elements. N_r can be significantly smaller than N_t and, in this case, the Rx must be able to resort to broader beams. The latter, asymmetrical case is particularly relevant when the Rx is an end user device.

The transmission is done over frequency selective channels. Let the channel be sampled with the sampling rate $f_s = 1/T_s$. The Rx symbol vector $\boldsymbol{y}[n] \in \mathbb{C}^{N_r}$ at the time instant nT_s is given as

$$\boldsymbol{y}[n] = \sum_{d=0}^{D} \boldsymbol{H}[d]\boldsymbol{x}[n-d] + \boldsymbol{z}[n], \tag{1}$$

where $\boldsymbol{x}[n] \in \mathbb{C}^{N_t}$, $\boldsymbol{z}[n] \in \mathbb{C}^{N_r}$, and $\boldsymbol{H}[n] \in \mathbb{C}^{N_r \times N_t}$ are the Tx vector, white Gaussian noise, and the matrix CIR sampled at the time instance nT_s, and D is the CIR length.

The system assumes block transmission where the Tx performs waveform (WF) processing and GP insertion. The discussion in the sequel will assume OFDM with N_{subc} subcarriers and the CP, but the results can be applied on other block based schemes, as well.

The Tx sends different data streams using Tx beams which are aligned with different physical paths. The number of streams is equal to the number of available RF chains N_{RF} at the Tx and Rx to simplify the exposition, and it is significantly smaller than the number of antenna elements. The BF can be realized in analog (e.g., as the first stage of the hybrid analog-digital architecture [8]) or digital domains, using subarray or fully connected architectures [1]. However, in all implementation cases, we assume the BF is fixed for the whole band of operation (i.e., all OFDM subcarriers) for complexity reasons. The role of the stream delay alignment block will be explained in Section III.

The receiver performs frequency independent Rx BF (again, with arbitrary implementation), followed by standard OFDM Rx processing including the CP removal, instantaneous effective MIMO channel estimation, and (fully digital) MIMO equalization.

The system equation for one OFDM subcarrier k can be written as

$$\hat{\boldsymbol{s}}_k = \boldsymbol{G}_k^{\mathrm{H}}\boldsymbol{G}_{\mathrm{BF}}^{\mathrm{H}}\boldsymbol{H}_k\boldsymbol{P}_{\mathrm{BF}}\boldsymbol{s}_k + \boldsymbol{G}_k^{\mathrm{H}}\boldsymbol{G}_{\mathrm{BF}}^{\mathrm{H}}\boldsymbol{z}_k, \quad k \in \{1, \ldots, N_{\text{subc}}\}, \tag{2}$$

where $\boldsymbol{s}_k \in \mathbb{C}^{N_{\mathrm{RF}}}$ and $\boldsymbol{x}_k = \boldsymbol{P}_{\mathrm{BF}}\boldsymbol{s}_k$, $\boldsymbol{x}_k \in \mathbb{C}^{N_t}$, are the symbol vector and the signal vector sent over the kth subcarrier, respectively. $\boldsymbol{z}_k \in \mathbb{C}^{N_r}$ is the Rx noise vector, $\hat{\boldsymbol{s}}_k$ is the estimated symbol vector, and $\boldsymbol{G}_k \in \mathbb{C}^{N_{\mathrm{RF}} \times N_{\mathrm{RF}}}$ is the Rx MIMO equalizer of the effective MIMO channel on subcarrier k. $\boldsymbol{G}_{\mathrm{BF}}^{\mathrm{H}} \in \mathbb{C}^{N_{\mathrm{RF}} \times N_r}$ and $\boldsymbol{P}_{\mathrm{BF}} \in \mathbb{C}^{N_t \times N_{\mathrm{RF}}}$ are the Rx and Tx beamformers, respectively.

As in any conventional block based transmission scheme, the GP length matches the effective channel delay spread. It will be discussed in the sequel that mmWave MIMO channels can have a large delay spread if no preprocessing is performed. The main goal of this paper is to show that these effective channel delay spreads can be reduced, rendering a more spectrally efficient transmission with shorter CPs.

ISBN 978-3-8007-4394-0

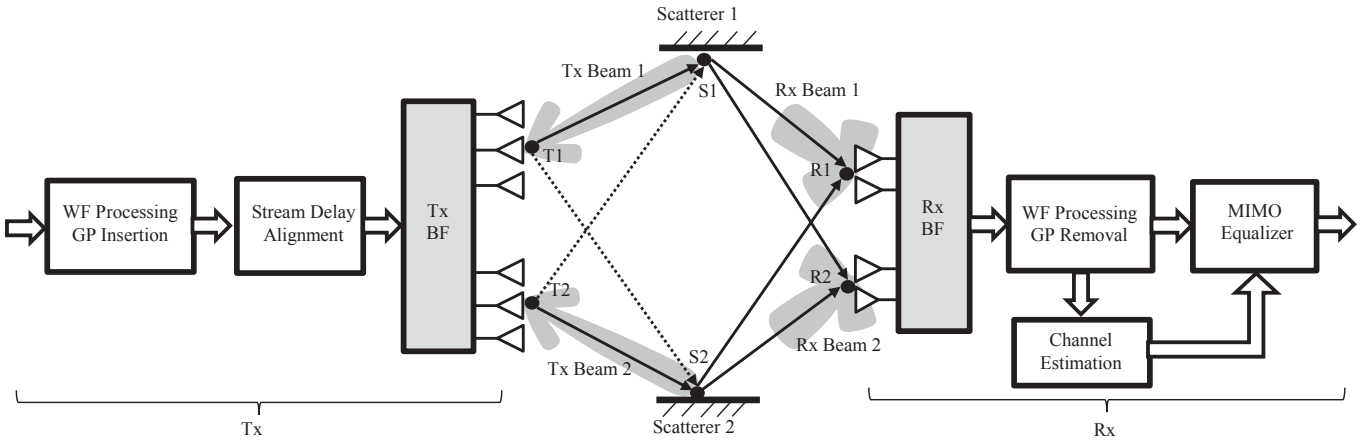

Fig. 1. System block scheme.

III. Channel Properties and Delay Alignment

A. Channel Related Aspects

The motivation for the proposed transceiver design comes from specific properties of the mmWave channel which can be summarized as follows. The mmWave channel exhibits sparsity, in the sense that it typically has only a few spatial lobes which carry the major part of signal energy [13]. This is a significant difference compared with sub-6 GHz wireless channels where more spatial richness can be observed. A few time clusters might appear in one lobe, but often only one is seen in mmWave channels.

An illustration of the concepts of spatial lobe and time cluster is shown in Fig. 2, while the supporting results from the measurement campaigns can be found, e.g., in [14]. A time cluster in mmWave channels contains typically a small number of resolvable paths [1]. One can conclude that the channel delay spreads inside one spatial lobe and especially inside one time cluster are significantly smaller compared with the total channel delay spread. Based on these observations, a more spectrally efficient mmWave MIMO transmission scheme is proposed in the sequel.

To simplify the exposition, we consider the case of a Tx sending two data streams $s^{(1)}[n]$ and $s^{(2)}[n]$ over combinations of different Tx and Rx spatial lobes defined by scatterers 1 and 2, as illustrated in Fig. 1, where each lobe combination corresponds to one time cluster. The spatial lobe combination 1 is geometrically defined by full line segments T1-S1 and S1-R1/R2. R1 or R2 can be used interchangeably as only large scale fading properties are relevant at the moment, and these are the same for both of these points. In fact, they can be considered quasi co-located for the subarray architecture case, and in the case of the fully connected architecture both points converge to one. Similarly, the spatial lobe combination 2 is geometrically defined by line segments T2-S2 and S2-R1/R2. It should be remarked that, the spatial lobes (time clusters) contain in general several different physical sub-paths, as described by the following channel equation

$$\boldsymbol{H}[d] = \sum_{c=1}^{N_\mathrm{c}} \sum_{p=1}^{N_\mathrm{path}^c} \alpha_{c,p}\rho(dT_s - \tau_c - \tau_p)\boldsymbol{a}_\mathrm{Rx}(\boldsymbol{\theta}_{c,p})\boldsymbol{a}_\mathrm{Tx}^\mathrm{H}(\boldsymbol{\phi}_{c,p}), \tag{3}$$

where N_c and N_path^c are the number of time clusters (in all lobes) and the number of paths in cluster c, respectively. $\alpha_{c,p}$ is the path gain for path p in cluster c, τ_c is the delay of the c-th cluster, τ_p is the delay of the p-th path within the cluster. $\boldsymbol{\theta}_{p,c}$ and $\boldsymbol{\phi}_{p,c}$ are the direction of arrival and departure vectors of path p within cluster c, respectively. ρ is the pulse-shaping filter. The vectors $\boldsymbol{a}_\mathrm{Tx}$ and $\boldsymbol{a}_\mathrm{Rx}$ are the antenna array response vectors for the Tx and Rx, respectively.

The propagation times over the spatial lobe combinations can be quite different, and in the example at hand we assume that the relative delay of the first cluster in the lobe combination T2-S2-R2 $\tau_c^{(2)}$, with respect to the delay of the first cluster in T1-S1-R1 $\tau_c^{(1)}$ is m samples, where the lobe combination 1 definition implicitly assumes

$$\|\boldsymbol{a}_\mathrm{Tx}(\boldsymbol{\phi}_{1,p})\|^2 \gg \boldsymbol{a}_\mathrm{Tx}^\mathrm{H}(\boldsymbol{\phi}_{1,p})\boldsymbol{a}_\mathrm{Tx}(\boldsymbol{\phi}_{2,p}), \quad \forall p, \tag{4}$$

$$\|\boldsymbol{a}_\mathrm{Rx}(\boldsymbol{\theta}_{1,p})\|^2 > \boldsymbol{a}_\mathrm{Rx}^\mathrm{H}(\boldsymbol{\theta}_{1,p})\boldsymbol{a}_\mathrm{Rx}(\boldsymbol{\theta}_{2,p}), \quad \forall p. \tag{5}$$

and similar relations hold for lobe combination 2. The quantitative meaning of the relation $\gg$ is discussed in Section III-B.

The delay spreads of the two lobe combinations are different too, and let the larger delay spread be l samples long. From the measurements and in the statistical channel models, m can be significantly larger than l. In other words, the total effective MIMO CIR might be rather long, while each of the spatial lobe combinations has on average a relatively small delay spread [13], [14].

The employed Tx and Rx beamforming create directional transmission where the stream $s^{(q)}[n]$ travels over spatial lobe combination q. If the Tx and Rx beams were extremely sharp, the scheme would result in two parallel data streams and the smaller terms in (4) and (5) could be neglected. In other words, almost no interstream interference would be present, and, after

ISBN 978-3-8007-4394-0

the WF processing, the Rx would see two differently delayed, independent data streams. While this might be a relevant case for backhaul transmission between the two macro BSs, we focus on the sequel on the more challenging case of imperfect BF due to reasonably large antenna arrays, particularly at the Rx side (end user device or small cell).

B. Interference Issues and Stream Delay Alignment

As depicted in Fig. 1, realistic BF leads to several issues.

- Rx side: Due to the limited hardware capabilities a more omnidirectional reception must be assumed. This means that the receive antennas collect simultaneously the signals stemming from the transmission of $s^{(1)}[n]$ over spatial lobe combination 1 and the delayed signals stemming from transmission of $s^{(2)}[n]$ over spatial lobe combination 2 and the difference between the terms in the inequality (5) is not so large.
- Tx side: Realistic Tx BF leads to some leakage of $s^{(1)}[n]$ transmission to the spatial lobe combination 2 (described by the smaller term in (4)) and vice versa. These interference directions are depicted by dotted lines T1-S2 and T2-S1 in Fig. 1. Similarly to the discussion above, T1 and T2 can be considered as quasi co-located (while S1 and S2 are not).

The Rx related issues are resolved by employing the Tx beam delay alignment block and Rx MIMO equalization. The beam delay alignment assumes delaying $s^{(1)}[n]$ by the estimated delay difference m between the two spatial lobe combinations. In other words,

$$s^{(1)}[n] \rightarrow s^{(1)}[n-m] \tag{6}$$

so the signals traveling though spatial lobe combination 1 arrive approximately at the same time as the signals using the spatial lobe combination 2. The Rx sees then a reduced effective MIMO CIR of length l and can apply standard OFDM Rx processing with the CP matched to the delay spread of the spatial lobe combination (and not the whole channel). In addition, the Rx can perform a convenient narrowband (per subcarrier) MIMO equalization technique to mitigate the interstream interference.

Regarding the Tx issue, as we assume macro BS as the Tx with a large antenna array, we opt to neglect the interference leakage in order to gain from the CIR shortening described above. We investigate the impact of this neglected interference by numerical simulations in Section IV, and realize that it can be tolerated in practice.

C. Notes on Channel Estimation

The proposed scheme can utilize a channel estimation procedure summarized as follows:

- The Tx and Rx exchange training packets in order to detect dominant channel paths and perform beam alignment, extending the methods of [6], and possibly in a hierarchical fashion (cf. e.g. [AH04]).

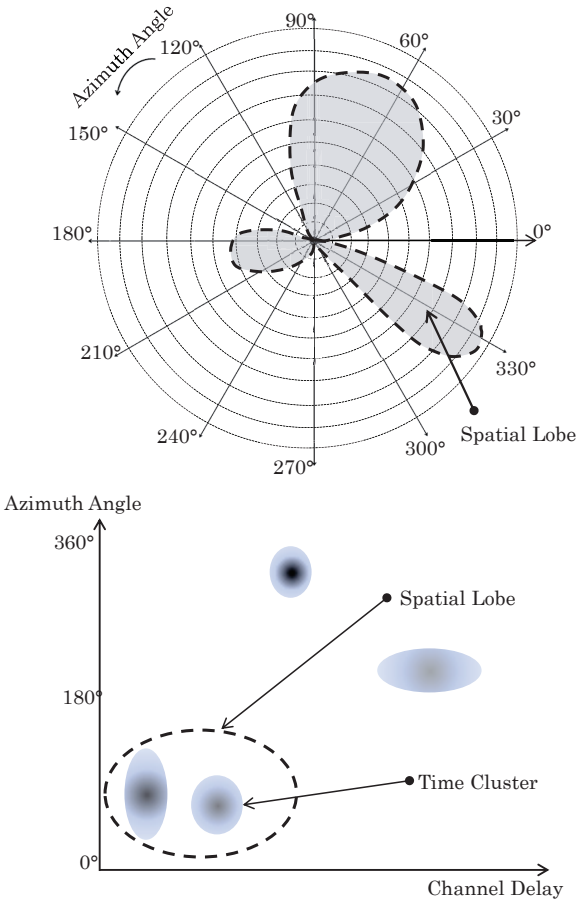

Fig. 2. Illustration of concepts of spatial lobe and time cluster. Upper part: Typical polar plot of the received power in the azimuth plane, where the power is proportional to the distance from the centre. Lower part: Typical power azimuth delay profile, where the power is proportional to the shade darkness.

- The Tx and Rx calculate the Tx and Rx beamformers, respectively, based on the available, partial (spatial) CSI, using a selected BF method.
- The Tx estimates the dominant path delays, either from the uplink training phase (in an TDD system) or via the feedback links from the Rx (in an FDD system).
- The Tx sends pilots for effective channel estimation at the Rx, utilized for Rx MIMO equalization. The effective channel can be seen as a convolution of the Rx BF, the radio channel, and the Tx BF.

It can be noted that the method can be adapted for both TDD and FDD type of systems. While the TDD mode is suitable due to channel reciprocity (possibly after applying calibration), the path delay information required at the Tx for the proposed scheme is not expected to change much in the two separate communication channels of FDD. As only approximate knowledge of path delays might be suffient for a significant CIR reduction, the technique can be considered as

ISBN 978-3-8007-4394-0

suitable for semi-open loop scenarios where only partial and relatively slowly changing information about the channel can be obtained at the Tx, e.g., due to the Doppler effect.

IV. Numerical Examples

The numerical evaluations are based on the implemented 2×2 (2 data streams) MIMO-OFDM link level simulation chain. The following system parameters and assumptions are used:

- The assumed carrier frequency is 30 GHz and the channel bandwidth is 100 MHz.
- The mmWave channel model is based on [15] assuming two scatterers for all investigated schemes, which are spatially separated ($\pm\pi/4$), while other channel parameters are unchanged. Only the spatially separated scatterers are taken into account for calculating the bit error rates as the nature of the method is adaptive. We remark that the modeling of path and cluster delays is aligned with the findings of [13].
- OFDM transmission assumes $N_{\mathrm{subc}} = 256$ subcarriers and different CP lengths depending on the analyzed method. The CP length covering the maximum channel delay spread is $\mathrm{CP}_{\mathrm{length}} = 107$ for the considered scenario.
- Subarray architecture is considered with 2 subarrays both at the Tx and Rx. Each subarray is realized as a uniform linear array and connected to one RF chain. Fixed Tx power constraint is assumed.
- Each of the two Rx subarrays has 8 antenna elements ($N_r = 16$ antenna elements in total at the Rx), while the number of antenna elements at the Tx is 64 or 128 per subarray ($N_t = 128$ or $N_t = 256$, respectively) in the simulations.
- Tx has limited CSI knowledge: Angles of the dominant paths (e.g., from a preceding beam alignment scheme), and approximated (threshold based) knowledge of delays of dominant paths are known.
- Ideal instantaneous CSI at Rx (an estimate would be obtained in practice through standard effective channel estimation process after the beam alignment, as described in Section III-C).
- Conventional Tx/Rx BF matching the angles of the dominant paths.
- Rx MIMO equalization as effective MIMO channel inversion

$$\boldsymbol{G}_k^{\mathrm{H}} = (\boldsymbol{G}_{\mathrm{BF}}^{\mathrm{H}} \boldsymbol{H}_k \boldsymbol{P}_{\mathrm{BF}})^{-1}, \quad k \in \{1, \ldots, N_{\mathrm{subc}}\}. \tag{7}$$

The overhead due to CP insertion is penalized in the SNR by a factor

$$F = 10 \log_{10} \frac{\mathrm{CP}_{\mathrm{length}} + N_{\mathrm{subc}}}{N_{\mathrm{subc}}} \quad [\mathrm{dB}], \tag{8}$$

analogously to the situations when comparing waveforms with different guard periods or with no guard periods (e.g., filterbank multi-carrier). Therefore, for the considered scenario the maximum possible saving (if there were no CP at all) is 1.52 dB.

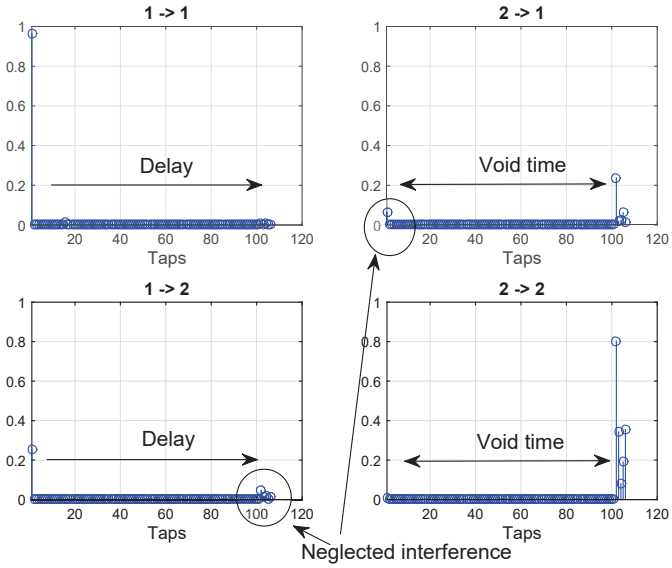

Fig. 3. Effective, normalized 2X2 MIMO CIR.

The methods compared in the simulation chain are:

- Baseline method 1: No stream delay alignment at the Tx and a sufficiently long CP applied to cover the maximum mmWave channel delay spread in the considered scenario.
- Baseline method 2: Methods utilizing no stream delay alignment at the Tx and having reduced CP lengths matching the delay spread of a spatial lobe combination.
- Proposed method: Reduced CP length to match the typical delay spread of a spatial lobe combination with stream delay alignment at the Tx.

To explain in more detail how the proposed scheme works, one illustrative MIMO channel realization, shown in Fig. 3, is taken as the first numerical example. The notation $\mathrm{A} \rightarrow \mathrm{B}$ means the channel from the Tx subarray A to the Rx subarray B. It can be noticed that there are large void times (sparsity in the time domain) in the effective channels which are eliminated by delaying of the streams. In the delaying operation, due to imperfect Tx BF a small portion of the interference is neglected. In Fig. 4, the effective MIMO channel impulse response is shown after delaying and shortening. It can be seen that the MIMO channel components are well aligned and that the overall CIR exhibits potential for a significant reduction of the CP.

The second numerical example, shown in Fig. 5, is a link level Monte Carlo simulation with a large number of MIMO channel realizations. One can notice that the proposed method outperforms the best baseline method by more than 1.3 dB in the case of uncoded Quadrature Phase Shift Keying (QPSK) transmission, for a very large SNR range. This corresponds to the CP overhead reduction or approximately 10 times enabled by operating on delay spreads of spatial lobe combinations (time clusters), and approaches the ideal value from (8). The

ISBN 978-3-8007-4394-0

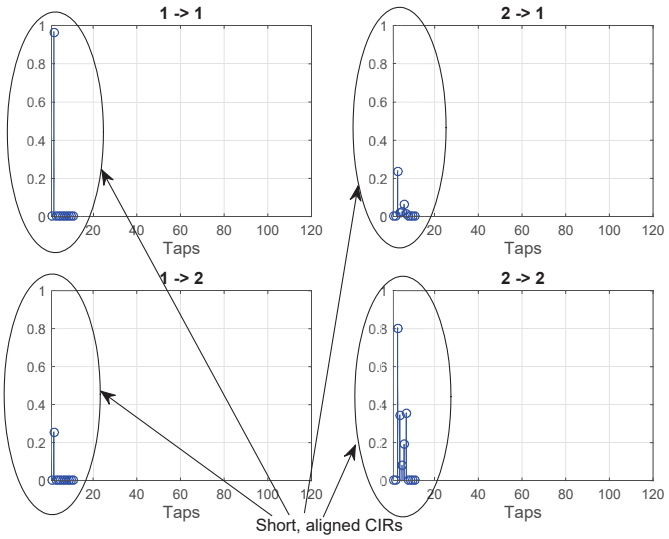

Fig. 4. Effective, normalized 2X2 MIMO CIR after delaying of the first stream and shortening of the whole MIMO CIR.

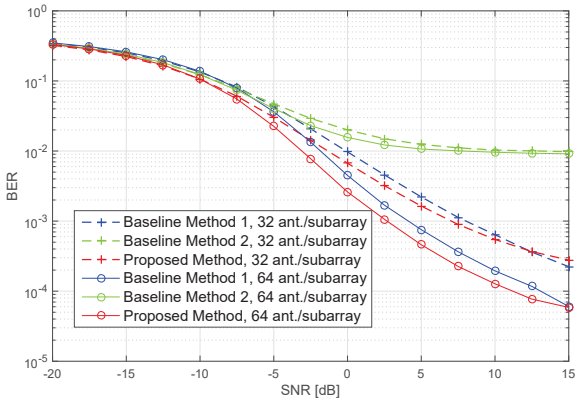

Fig. 5. BER vs. the SNR for the proposed and the baseline methods.

results are valid for both investigated Tx antenna arrays, while one can observe that utilizing larger arrays shifts the crossing point between the proposed and the long CP method to higher SNR regions. This effect can be expected as the Tx BF interference leakage is smaller in this case. As seen in Fig. 5, the effect of neglected interference due to imperfect Tx BF is visible only at very high SNRs of little practical interest for mmWave communication, since typical operating points are likely to be (significantly) below 10 dB.

V. Conclusion

It is shown how specific mmWave channel properties can be exploited for a significant reduction of the effective MIMO CIR in cases when the signals propagate over different physical paths. With a semi-open loop scheme that pre-compensates the path delays, the multiple streams arrive at approximately the same time at the receiver, and the guard periods of block transmission schemes can thus be significantly reduced with only partial transmit CSI.

Acknowledgment

The research leading to these results has received funding from the European Union Horizon 2020 research and innovation programme under grant agreement No 671551 (5G-XHaul). The European Union and its agencies are not liable or otherwise responsible for the contents of this document; its content reflects the view of its authors only.

References

[1] T. S. Rappaport, R. W. Heath, Jr., R. C. Daniels, and J. N. Murdock, *Millimeter Wave Wireless Communications*. Upper Saddle River, NJ, USA: Prentice Hall, 2015.

[2] N. Al-Dhahir, "FIR channel-shortening equalizers for MIMO ISI channels," *IEEE Trans. Commun.*, vol. 49, no. 2, pp. 231–218, Feb. 2001.

[3] M. B. Breinholt, M. D. Zoltowski, and T. A. Thomas, "Space-time equalization and interference cancellation for MIMO OFDM," in *Proc. 36th Asilomar Conference on Signals, Systems and Computers*, Pacific Grove, CA, USA, Nov. 2002, pp. 1688–1693.

[4] S. Badri-Hoeher, P. A. Hoeher, C. Krakowski, and W. Xu, "Impulse response shortening for multiple co-channels," in *Proc. IEEE International Conference on Communications 2005 (ICC'05)*, Seoul, Korea, May 2005, pp. 1896–1900.

[5] R. Samanta, R. W. Heath, Jr., and B. L. Evans, "Joint interference cancellation and channel shortening in multiuser-MIMO systems," *IEEE Trans. Veh. Techn.*, vol. 56, no. 2, pp. 652–660, Mar. 2007.

[6] IEEE 802.11 Working Group, *Part 11: Wireless LAN Medium Access Control (MAC) and Physical Layer (PHY) Specifications IEEE 802.11ad*, Jan. 2012, amendment 3: Enhancements for Very High Throughput in the 60 GHz Band.

[7] 3rd Generation Partnership Project, *Study on Scenarios and Requirements for Next Generation Access Technologies, 3GPP TR 38.913 v.14.0.0*, Oct. 2016.

[8] A. Alkhateeb and R. W. Heath, Jr., "Frequency selective hybrid precoding for limited feedback millimeter wave systems," *IEEE Trans. Commun.*, vol. 4, no. 5, pp. 1801–1818, May 2016.

[9] G. Wang, P. Karanjekar, and G. Ascheid, "Beamforming with time-delay compensation for 60 GHz MIMO frequency-selective channels," in *Proc. IEEE PIMRC 2015*, Hong Kong, China, Sep. 2015.

[10] Y. Zeng and R. Zhang, "Millimeter wave MIMO with lens antenna array: A new path division multiplexing paradigm," *IEEE Trans. Commun.*, vol. 64, pp. 1557–1571, Apr. 2016.

[11] M.-A. Bouzigues, I. Siaud, M. Helard, and A.-M. Ulmer-Moll, "Turn back the clock: Time reversal for green radio communications," *IEEE Veh. Technol. Mag.*, vol. 8, pp. 49–56, Mar. 2013.

[12] C. A. Viteri-Mera and F. L. Teixeira, "Interference-nulling time-reversal beamforming for mm-wave massive MIMO in multi-user frequency-selective indoor channels," Jul. 2015, arxiv: 1506.05143v2.

[13] M. K. Samimi and T. S. Rappaport, "Ultra-wideband statistical channel model for non line of sight millimeter-wave urban channels," in *Proc. Globecom 2014*, Austin, TX, USA, Dec. 2014, pp. 3483–3489.

[14] D. Dupleich, S. Häfner, C. Schneider, R. Müller, R. Thomä, J. Luo, N. Iqbal, E. Schulz, X. Lu, and G. Wang, "Double-directional and dual-polarimetric indoor measurements at 70 GHz," in *Proc. PIMRC 2015*, Hong Kong, China, Sep. 2015, pp. 2234 – 2238.

[15] M. Iwanow, N. Vucic, M. Castaneda, J. Luo, W. Xu, and W. Utschick, "Some aspects on hybrid wideband transceiver design for mmWave communication systems," in *Proc. WSA 2016; 20th Int. ITG Workshop Smart Antennas*, Munich, Germany, Mar. 2016, pp. 1–8.

